Search for new π[superscript 0]-like particles produced in association with a #-lepton pair

Search for new π^0-like particles produced in association with a τ-lepton pair

J. P. Lees,[1] V. Poireau,[1] V. Tisserand,[1] E. Grauges,[2] A. Palano,[3a,3b] G. Eigen,[4] B. Stugu,[4] D. N. Brown,[5] L. T. Kerth,[5] Yu. G. Kolomensky,[5] M. J. Lee,[5] G. Lynch,[5] H. Koch,[6] T. Schroeder,[6] C. Hearty,[7] T. S. Mattison,[7] J. A. McKenna,[7] R. Y. So,[7] A. Khan,[8] V. E. Blinov,[9a,9b,9c] A. R. Buzykaev,[9a] V. P. Druzhinin,[9a,9b] V. B. Golubev,[9a,9b] E. A. Kravchenko,[9a,9b] A. P. Onuchin,[9a,9b,9c] S. I. Serednyakov,[9a,9b] Yu. I. Skovpen,[9a,9b] E. P. Solodov,[9a,9b] K. Yu. Todyshev,[9a,9b] A. J. Lankford,[10] M. Mandelkern,[10] B. Dey,[11] J. W. Gary,[11] O. Long,[11] C. Campagnari,[12] M. Franco Sevilla,[12] T. M. Hong,[12] D. Kovalskyi,[12] J. D. Richman,[12] C. A. West,[12] A. M. Eisner,[13] W. S. Lockman,[13] W. Panduro Vazquez,[13] B. A. Schumm,[13] A. Seiden,[13] D. S. Chao,[14] C. H. Cheng,[14] B. Echenard,[14] K. T. Flood,[14] D. G. Hitlin,[14] T. S. Miyashita,[14] P. Ongmongkolkul,[14] F. C. Porter,[14] M. Röhrken,[14] R. Andreassen,[15] Z. Huard,[15] B. T. Meadows,[15] B. G. Pushpawela,[15] M. D. Sokoloff,[15] L. Sun,[15] P. C. Bloom,[16] W. T. Ford,[16] A. Gaz,[16] J. G. Smith,[16] S. R. Wagner,[16] R. Ayad,[17,†] W. H. Toki,[17] B. Spaan,[18] D. Bernard,[19] M. Verderi,[19] S. Playfer,[20] D. Bettoni,[21a] C. Bozzi,[21a] R. Calabrese,[21a,21b] G. Cibinetto,[21a,21b] E. Fioravanti,[21a,21b] I. Garzia,[21a,21b] E. Luppi,[21a,21b] L. Piemontese,[21a] V. Santoro,[21a] A. Calcaterra,[22] R. de Sangro,[22] G. Finocchiaro,[22] S. Martellotti,[22] P. Patteri,[22] I. M. Peruzzi,[22,‡] M. Piccolo,[22] M. Rama,[22] A. Zallo,[22] R. Contri,[23a,23b] M. Lo Vetere,[23a,23b] M. R. Monge,[23a,23b] S. Passaggio,[23a] C. Patrignani,[23a,23b] E. Robutti,[23a] B. Bhuyan,[24] V. Prasad,[24] A. Adametz,[25] U. Uwer,[25] H. M. Lacker,[26] U. Mallik,[27] C. Chen,[28] J. Cochran,[28] S. Prell,[28] H. Ahmed,[29] A. V. Gritsan,[30] N. Arnaud,[31] M. Davier,[31] D. Derkach,[31] G. Grosdidier,[31] F. Le Diberder,[31] A. M. Lutz,[31] B. Malaescu,[31,§] P. Roudeau,[31] A. Stocchi,[31] G. Wormser,[31] D. J. Lange,[32] D. M. Wright,[32] J. P. Coleman,[33] J. R. Fry,[33] E. Gabathuler,[33] D. E. Hutchcroft,[33] D. J. Payne,[33] C. Touramanis,[33] A. J. Bevan,[34] F. Di Lodovico,[34] R. Sacco,[34] G. Cowan,[35] J. Bougher,[36] D. N. Brown,[36] C. L. Davis,[36] A. G. Denig,[37] M. Fritsch,[37] W. Gradl,[37] K. Griessinger,[37] A. Hafner,[37] K. R. Schubert,[37] R. J. Barlow,[38,‖] G. D. Lafferty,[38] R. Cenci,[39] B. Hamilton,[39] A. Jawahery,[39] D. A. Roberts,[39] R. Cowan,[40] G. Sciolla,[40] R. Cheaib,[41] P. M. Patel,[41,*] S. H. Robertson,[41] N. Neri,[42a] F. Palombo,[42a,42b] L. Cremaldi,[43] R. Godang,[43,¶] P. Sonnek,[43] D. J. Summers,[43] M. Simard,[44] P. Taras,[44] G. De Nardo,[45a,45b] G. Onorato,[45a,45b] C. Sciacca,[45a,45b] M. Martinelli,[46] G. Raven,[46] C. P. Jessop,[47] J. M. LoSecco,[47] K. Honscheid,[48] R. Kass,[48] E. Feltresi,[49a,49b] M. Margoni,[49a,49b] M. Morandin,[49a] M. Posocco,[49a] M. Rotondo,[49a] G. Simi,[49a,49b] F. Simonetto,[49a,49b] R. Stroili,[49a,49b] S. Akar,[50] E. Ben-Haim,[50] M. Bomben,[50] G. R. Bonneaud,[50] H. Briand,[50] G. Calderini,[50] J. Chauveau,[50] Ph. Leruste,[50] G. Marchiori,[50] J. Ocariz,[50] M. Biasini,[51a,51b] E. Manoni,[51a] S. Pacetti,[51a,51b] A. Rossi,[51a] C. Angelini,[52a,52b] G. Batignani,[52a,52b] S. Bettarini,[52a,52b] M. Carpinelli,[52a,52b,**] G. Casarosa,[52a,52b] A. Cervelli,[52a,52b] M. Chrzaszcz,[52a] F. Forti,[52a,52b] M. A. Giorgi,[52a,52b] A. Lusiani,[52a,52c] B. Oberhof,[52a,52b] E. Paoloni,[52a,52b] A. Perez,[52a] G. Rizzo,[52a,52b] J. J. Walsh,[52a] D. Lopes Pegna,[53] J. Olsen,[53] A. J. S. Smith,[53] R. Faccini,[54a,54b] F. Ferrarotto,[54a] F. Ferroni,[54a,54b] M. Gaspero,[54a,54b] L. Li Gioi,[54a] A. Pilloni,[54a,54b] G. Piredda,[54a] C. Bünger,[55] S. Dittrich,[55] O. Grünberg,[55] M. Hess,[55] T. Leddig,[55] C. Voß,[55] R. Waldi,[55] T. Adye,[56] E. O. Olaiya,[56] F. F. Wilson,[56] S. Emery,[57] G. Vasseur,[57] F. Anulli,[58,††] D. Aston,[58] D. J. Bard,[58] C. Cartaro,[58] M. R. Convery,[58] J. Dorfan,[58] G. P. Dubois-Felsmann,[58] W. Dunwoodie,[58] M. Ebert,[58] R. C. Field,[58] B. G. Fulsom,[58] M. T. Graham,[58] C. Hast,[58] W. R. Innes,[58] P. Kim,[58] D. W. G. S. Leith,[58] P. Lewis,[58] D. Lindemann,[58] S. Luitz,[58] V. Luth,[58] H. L. Lynch,[58] D. B. MacFarlane,[58] D. R. Muller,[58] H. Neal,[58] M. Perl,[58,*] T. Pulliam,[58] B. N. Ratcliff,[58] A. Roodman,[58] A. A. Salnikov,[58] R. H. Schindler,[58] A. Snyder,[58] D. Su,[58] M. K. Sullivan,[58] J. Va'vra,[58] W. J. Wisniewski,[58] H. W. Wulsin,[58] M. V. Purohit,[59] R. M. White,[59,‡‡] J. R. Wilson,[59] A. Randle-Conde,[60] S. J. Sekula,[60] M. Bellis,[61] P. R. Burchat,[61] E. M. T. Puccio,[61] M. S. Alam,[62] J. A. Ernst,[62] R. Gorodeisky,[63] N. Guttman,[63] D. R. Peimer,[63] A. Soffer,[63] S. M. Spanier,[64] J. L. Ritchie,[65] R. F. Schwitters,[65] B. C. Wray,[65] J. M. Izen,[66] X. C. Lou,[66] F. Bianchi,[67a,67b] F. De Mori,[67a,67b] A. Filippi,[67a] D. Gamba,[67a,67b] L. Lanceri,[68a,68b] L. Vitale,[68a,68b] F. Martinez-Vidal,[69] A. Oyanguren,[69] P. Villanueva-Perez,[69] J. Albert,[70] Sw. Banerjee,[70] A. Beaulieu,[70] F. U. Bernlochner,[70] H. H. F. Choi,[70] G. J. King,[70] R. Kowalewski,[70] M. J. Lewczuk,[70] T. Lueck,[70] D. McKeen,[70,§§] I. M. Nugent,[70] M. Pospelov,[70,‖‖] J. M. Roney,[70] R. J. Sobie,[70] N. Tasneem,[70] T. J. Gershon,[71] P. F. Harrison,[71] T. E. Latham,[71] H. R. Band,[72] S. Dasu,[72] Y. Pan,[72] R. Prepost,[72] and S. L. Wu[72]

(*BABAR* Collaboration)

[1]*Laboratoire d'Annecy-le-Vieux de Physique des Particules (LAPP), Université de Savoie, CNRS/IN2P3, F-74941 Annecy-Le-Vieux, France*
[2]*Universitat de Barcelona, Facultat de Fisica, Departament ECM, E-08028 Barcelona, Spain*
[3a]*INFN Sezione di Bari, I-70126 Bari, Italy*
[3b]*Dipartimento di Fisica, Università di Bari, I-70126 Bari, Italy*
[4]*University of Bergen, Institute of Physics, N-5007 Bergen, Norway*
[5]*Lawrence Berkeley National Laboratory and University of California, Berkeley, California 94720, USA*
[6]*Ruhr Universität Bochum, Institut für Experimentalphysik 1, D-44780 Bochum, Germany*
[7]*University of British Columbia, Vancouver, British Columbia, Canada V6T 1Z1*
[8]*Brunel University, Uxbridge, Middlesex UB8 3PH, United Kingdom*
[9a]*Budker Institute of Nuclear Physics SB RAS, Novosibirsk 630090, Russia*

[9b]*Novosibirsk State University, Novosibirsk 630090, Russia*
[9c]*Novosibirsk State Technical University, Novosibirsk 630092, Russia*
[10]*University of California at Irvine, Irvine, California 92697, USA*
[11]*University of California at Riverside, Riverside, California 92521, USA*
[12]*University of California at Santa Barbara, Santa Barbara, California 93106, USA*
[13]*University of California at Santa Cruz, Institute for Particle Physics, Santa Cruz, California 95064, USA*
[14]*California Institute of Technology, Pasadena, California 91125, USA*
[15]*University of Cincinnati, Cincinnati, Ohio 45221, USA*
[16]*University of Colorado, Boulder, Colorado 80309, USA*
[17]*Colorado State University, Fort Collins, Colorado 80523, USA*
[18]*Technische Universität Dortmund, Fakultät Physik, D-44221 Dortmund, Germany*
[19]*Laboratoire Leprince-Ringuet, Ecole Polytechnique, CNRS/IN2P3, F-91128 Palaiseau, France*
[20]*University of Edinburgh, Edinburgh EH9 3JZ, United Kingdom*
[21a]*INFN Sezione di Ferrara, I-44122 Ferrara, Italy*
[21b]*Dipartimento di Fisica e Scienze della Terra, Università di Ferrara, I-44122 Ferrara, Italy*
[22]*INFN Laboratori Nazionali di Frascati, I-00044 Frascati, Italy*
[23a]*INFN Sezione di Genova, I-16146 Genova, Italy*
[23b]*Dipartimento di Fisica, Università di Genova, I-16146 Genova, Italy*
[24]*Indian Institute of Technology Guwahati, Guwahati, Assam 781 039, India*
[25]*Universität Heidelberg, Physikalisches Institut, D-69120 Heidelberg, Germany*
[26]*Humboldt-Universität zu Berlin, Institut für Physik, D-12489 Berlin, Germany*
[27]*University of Iowa, Iowa City, Iowa 52242, USA*
[28]*Iowa State University, Ames, Iowa 50011-3160, USA*
[29]*Physics Department, Jazan University, Jazan 22822, Kingdom of Saudi Arabia*
[30]*Johns Hopkins University, Baltimore, Maryland 21218, USA*
[31]*Laboratoire de l'Accélérateur Linéaire, IN2P3/CNRS et Université Paris-Sud 11, Centre Scientifique d'Orsay, F-91898 Orsay Cedex, France*
[32]*Lawrence Livermore National Laboratory, Livermore, California 94550, USA*
[33]*University of Liverpool, Liverpool L69 7ZE, United Kingdom*
[34]*Queen Mary, University of London, London, E1 4NS, United Kingdom*
[35]*University of London, Royal Holloway and Bedford New College, Egham, Surrey TW20 0EX, United Kingdom*
[36]*University of Louisville, Louisville, Kentucky 40292, USA*
[37]*Johannes Gutenberg-Universität Mainz, Institut für Kernphysik, D-55099 Mainz, Germany*
[38]*University of Manchester, Manchester M13 9PL, United Kingdom*
[39]*University of Maryland, College Park, Maryland 20742, USA*
[40]*Massachusetts Institute of Technology, Laboratory for Nuclear Science, Cambridge, Massachusetts 02139, USA*
[41]*McGill University, Montréal, Québec, Canada H3A 2T8*
[42a]*INFN Sezione di Milano, I-20133 Milano, Italy*
[42b]*Dipartimento di Fisica, Università di Milano, I-20133 Milano, Italy*
[43]*University of Mississippi, University, Mississippi 38677, USA*
[44]*Université de Montréal, Physique des Particules, Montréal, Québec, Canada H3C 3J7*
[45a]*INFN Sezione di Napoli, I-80126 Napoli, Italy*
[45b]*Dipartimento di Scienze Fisiche, Università di Napoli Federico II, I-80126 Napoli, Italy*
[46]*NIKHEF, National Institute for Nuclear Physics and High Energy Physics, NL-1009 DB Amsterdam, The Netherlands*
[47]*University of Notre Dame, Notre Dame, Indiana 46556, USA*
[48]*Ohio State University, Columbus, Ohio 43210, USA*
[49a]*INFN Sezione di Padova, I-35131 Padova, Italy*
[49b]*Dipartimento di Fisica, Università di Padova, I-35131 Padova, Italy*
[50]*Laboratoire de Physique Nucléaire et de Hautes Energies, IN2P3/CNRS, Université Pierre et Marie Curie-Paris6, Université Denis Diderot-Paris7, F-75252 Paris, France*
[51a]*INFN Sezione di Perugia, I-06123 Perugia, Italy*
[51b]*Dipartimento di Fisica, Università di Perugia, I-06123 Perugia, Italy*
[52a]*INFN Sezione di Pisa, I-56127 Pisa, Italy*
[52b]*Dipartimento di Fisica, Università di Pisa, I-56127 Pisa, Italy*
[52c]*Scuola Normale Superiore di Pisa, I-56127 Pisa, Italy*
[53]*Princeton University, Princeton, New Jersey 08544, USA*
[54a]*INFN Sezione di Roma, I-00185 Roma, Italy*

[54b]Dipartimento di Fisica, Università di Roma La Sapienza, I-00185 Roma, Italy
[55]Universität Rostock, D-18051 Rostock, Germany
[56]Rutherford Appleton Laboratory, Chilton, Didcot, Oxon OX11 0QX, United Kingdom
[57]CEA, Irfu, SPP, Centre de Saclay, F-91191 Gif-sur-Yvette, France
[58]SLAC National Accelerator Laboratory, Stanford, California 94309, USA
[59]University of South Carolina, Columbia, South Carolina 29208, USA
[60]Southern Methodist University, Dallas, Texas 75275, USA
[61]Stanford University, Stanford, California 94305-4060, USA
[62]State University of New York, Albany, New York 12222, USA
[63]Tel Aviv University, School of Physics and Astronomy, Tel Aviv 69978, Israel
[64]University of Tennessee, Knoxville, Tennessee 37996, USA
[65]University of Texas at Austin, Austin, Texas 78712, USA
[66]University of Texas at Dallas, Richardson, Texas 75083, USA
[67a]INFN Sezione di Torino, I-10125 Torino, Italy
[67b]Dipartimento di Fisica, Università di Torino, I-10125 Torino, Italy
[68a]INFN Sezione di Trieste, I-34127 Trieste, Italy
[68b]Dipartimento di Fisica, Università di Trieste, I-34127 Trieste, Italy
[69]IFIC, Universitat de Valencia-CSIC, E-46071 Valencia, Spain
[70]University of Victoria, Victoria, British Columbia, Canada V8W 3P6
[71]Department of Physics, University of Warwick, Coventry CV4 7AL, United Kingdom
[72]University of Wisconsin, Madison, Wisconsin 53706, USA
(Received 11 November 2014; published 23 December 2014)

We report on a search in e^+e^- annihilations for new π^0-like particles produced in association with a τ-lepton pair. These objects, with a similar mass and similar decay modes to π^0 mesons, could provide an explanation for the non-asymptotic behavior of the pion-photon transition form factor observed by the *BABAR* Collaboration. No significant signal is observed, and limits on the production cross section at the level of 73 fb or 370 fb, depending on the model parameters, are determined at 90% confidence level. These upper limits lie below the cross section values needed to explain the *BABAR* form factor data.

DOI: 10.1103/PhysRevD.90.112011 PACS numbers: 14.40.Rt, 14.60.Fg

I. INTRODUCTION

The measurement of the pion-photon transition form factor $\mathcal{F}_{\pi^0}(Q^2)$ reported by the *BABAR* Collaboration [1] has given rise to much discussion [2–5]. The result does not exhibit convergence towards the Brodsky-Lepage limit of 185 MeV$/Q^2$ [6] even for large values of the squared momentum transfer, viz., $Q^2 > 15$ GeV^2, where the data are expected to be well described by perturbative QCD. Results from the Belle Collaboration [7] show better agreement with the perturbative predictions but are consistent with the *BABAR* data within the uncertainties.

A recent suggestion [8] proposes that the observed lack of asymptotic behavior might be due to the production of new particles or states, tentatively named "pion impostors" and generically denoted ϕ [9]. Two classes of models are considered. In the first, scalar ϕ_S or pseudoscalar ϕ_P particles are introduced with a mass within 10 MeV$/c^2$ of the π^0 mass, and with similar decay modes to the π^0, such that they thereby contribute to the $\mathcal{F}_{\pi^0}(Q^2)$ measurement. In the second, a new light pseudoscalar state mixes with the π^0 to produce a so-called "hardcore pion" $\pi^0_{\rm HC}$. The ϕ_P and $\pi^0_{\rm HC}$ have similar experimental signatures and the related processes only differ in their production rates. These models predict large coupling strengths between the new objects and the τ lepton, comparable to the strength of the strong force, leading to an observable increase of $\mathcal{F}_{\pi^0}(Q^2)$ through virtual loops with τ leptons. The couplings of the new particles to heavy quarks and other Standard Model (SM) particles are constrained by experimental data to be an order of magnitude or more smaller [8].

The largeness of the predicted couplings of the pion impostors to the τ lepton, and the absence of corresponding

[*]Deceased.
[†]Present address: University of Tabuk, Tabuk 71491, Saudi Arabia.
[‡]Also at: Università di Perugia, Dipartimento di Fisica, I-06123 Perugia, Italy.
[§]Present address: Laboratoire de Physique Nucléaire et de Hautes Energies, IN2P3/CNRS, F-75252 Paris, France.
[‖]Present address: University of Huddersfield, Huddersfield HD1 3DH, United Kingdom.
[¶]Present address: University of South Alabama, Mobile, Alabama 36688, USA.
[**]Also at: Università di Sassari, I-07100 Sassari, Italy.
[††]Also at: INFN Sezione di Roma, I-00185 Roma, Italy.
[‡‡]Present address: Universidad Técnica Federico Santa Maria, 2390123 Valparaiso, Chile.
[§§]Present address: University of Washington, Seattle, Washington 98195, USA.
[‖‖]Also at: Perimeter Institute for Theoretical Physics, Waterloo, Ontario, Canada N2J 2W9.

TABLE I. Production cross sections of $e^+e^- \to \tau^+\tau^-\pi^0_{\rm HC}$, $\tau^+\tau^-\phi_P$, and $\tau^+\tau^-\phi_S$ at $\sqrt{s} = 10.58$ GeV needed to accommodate the pion-photon transition form factor reported by *BABAR*, as well as the combination of *BABAR* and Belle measurements. Confidence intervals at 95% confidence level are provided in brackets.

Model	σ (pb) *BABAR* [1]		σ (pb) *BABAR* + Belle [7]	
$\pi^0_{\rm HC}$	0.62	[0.25–0.84]	0.44	[0.15–0.59]
ϕ_P	4.8	[2.5–6.9]	3.4	[2.5–5.1]
ϕ_S	130	[70–180]	90	[50–140]

experimental constraints, motivate a search for pion impostors radiated from τ leptons in $e^+e^- \to \tau^+\tau^-\phi$, $\phi \to \gamma\gamma$ interactions. This process is particularly compelling because the rate of such events must be considerable in order to explain the *BABAR* $\mathcal{F}_{\pi^0}(Q^2)$ data, making it potentially observable. The production cross sections required to describe the *BABAR* measurements are listed in Table I. The corresponding results for the combined *BABAR* and Belle data are also given. Based on the cross sections derived from the *BABAR* data alone, on the order of 10^5 events are expected in the *BABAR* data sample.

The SM production of genuine π^0 meson in association with a τ-lepton pair is expected to be highly suppressed. To lowest order, the SM process in which a π^0 is radiated from a τ lepton is depicted in Fig. 1. The matrix element involves the pseudoscalar to two-photon transition amplitude as well as a suppression factor arising from the two-photon loop and the τ-lepton propagator. The matrix element for this diagram [10,11] yields an effective coupling between the π^0 and the τ lepton of the form

$$g^{\rm e.m.}_{\tau\tau} = -\frac{1}{\sqrt{2}}\frac{m_\tau}{f_\pi}\left(\frac{\alpha}{\pi}\right)^2 R, \tag{1}$$

where m_τ is the mass of the τ lepton, $f_\pi \simeq 0.130$ GeV is the pion decay constant, and α is the fine-structure constant. The factor R is a dimensionless complex amplitude that is a function of the pion form factor $\mathcal{F}_{\pi^0}(k^2, (p_{\pi^0} - k)^2)$, integrated over the virtual photon four-momentum k, and of the mass ratio m_τ/m_{π^0} between the τ lepton and the neutral pion. Using a simplified analytical expression for the form factor [10], the magnitude of R is estimated to be around 0.2. The SM electromagnetic τ-π^0 coupling is therefore

$$|g^{\rm e.m.}_{\tau\tau}| \sim \mathcal{O}(10^{-5}), \tag{2}$$

which is approximately four orders of magnitude smaller than the coupling strength expected for the impostor model.

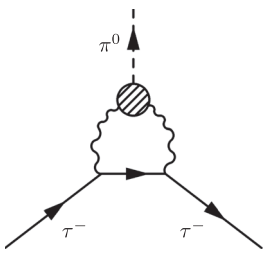

FIG. 1. Diagram of the leading order SM process for π^0 radiation from a τ lepton.

A second potential SM background arises from events in which the π^0 meson is created through the s-channel virtual photon from the e^+e^- annihilation, together with another photon that converts to a τ-lepton pair. This process is highly suppressed by the form factor at $Q^2 = (10.58\,\text{GeV})^2$. Compared to the τ-lepton pair rate, it is further suppressed by a factor of α.

The total combined expected background yield from the two SM background processes described above corresponds to less than around 0.01 events, which is negligible compared to the number of pion impostor events required to explain the $\mathcal{F}_{\pi^0}(Q^2)$ anomaly.

We present a search for new π^0-like particles in the $e^+e^- \to \tau^+\tau^-\phi$ final state, where ϕ can be any of the ϕ_P, ϕ_S, or $\pi^0_{\rm HC}$ states. The paper is organized as follows: Sec. II describes the detector and data samples used in this analysis, while Sec. III presents the signal selection and the yield extraction methodology. The main contributions to the systematic uncertainty are described in Sec. IV and the results are presented in Sec. V. Section VI contains a summary.

II. THE *BABAR* DETECTOR, DATA AND SIMULATION

The data used in this analysis were collected with the *BABAR* detector at the PEP-II asymmetric-energy e^+e^- storage rings between 1999 and 2007. The *BABAR* detector is described in detail elsewhere [12,13]. Here we provide a brief overview of the two subdetectors most relevant to this analysis.

The energy of photons and electrons is measured with an electromagnetic calorimeter (EMC) composed of a cylindrical array of CsI(Tl) crystals. The resolution for the polar and azimuthal angles is ~4 mrad, and the energy resolution is ~3% for 1 GeV photons [12]. The EMC also serves as a particle identification (PID) device for electrons. The drift chamber is used to determine the momentum of the charged tracks by measuring their curvature in a 1.5 T magnetic field. The transverse momentum resolution is a linear function of the transverse momentum p_T and is 0.67% for $p_T = 1.7$ GeV/c, which is the mean laboratory p_T value of charged tracks expected in signal events.

This analysis is based on 424 fb^{-1} of data collected at a center-of-mass (CM) energy $\sqrt{s} = 10.58$ GeV and on 44 fb^{-1} collected at $\sqrt{s} = 10.54$ GeV [14], corresponding to a total production of approximately 430×10^6 $\tau^+\tau^-$ pairs.

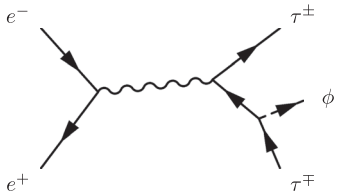

FIG. 2. Diagram of the pion impostor production process in e^+e^- annihilations. The ϕ can be any of the ϕ_P, ϕ_S, or $\pi^0_{\rm HC}$ particles.

Simulated signal events are created using the EvtGen [15] generator. First, large samples of $e^+e^- \to \tau^+\tau^-\pi^0$ events are generated, based on three-body phase space and nominal decay modes for the τ leptons and π^0 meson. Then the events are reweighted to reflect the production rate of $e^+e^- \to \tau^+\tau^-\phi$ processes using the analytical matrix elements corresponding to the pion impostor process illustrated in Fig. 2, assuming either the scalar or pseudoscalar hypothesis.

The following backgrounds are considered: $e^+e^- \to B\bar{B}$ events, generated with the EvtGen [15] program, continuum hadronic $e^+e^- \to q\bar{q}(q = u, d, s, c)$ events, generated with the JETSET [16] program, $e^+e^- \to \mu^+\mu^-$ and $e^+e^- \to \tau^+\tau^-$ events, generated with the $\mathcal{KK}$ [17] program, with the decay of the τ leptons described using the TAUOLA [18] library, and $e^+e^- \to e^+e^-$ events are simulated with the BHWIDE [19] program. Radiative corrections are modeled with the PHOTOS [20] algorithm and the detector response with the GEANT4 [21] toolkit.

III. ANALYSIS METHOD

The signal consists of a $\tau^+\tau^-$ pair and a single pion impostor ϕ. The pion impostor decays to a pair of photons with diphoton invariant mass close to the π^0 mass. The selection criteria are optimized using simulated signal and background events. Simulated samples are also used to evaluate the selection efficiency and systematic uncertainties. These quantities are evaluated using an impostor mass set equal to the mass of the π^0.

A. Signal selection

For the selection of $e^+e^- \to \tau^+\tau^-\phi$ signal events, we require one τ lepton to decay leptonically to an electron and the other to a muon. This requirement suppresses background from radiative Bhabha and dimuon events. We thus require events to contain exactly two charged tracks, one identified as an electron and the other as a muon. To reduce background from two-photon $e^+e^- \to e^+e^-X$ events, signal event candidates are required to have a missing transverse momentum larger than 0.3 GeV/c, where the missing transverse momentum is the magnitude of the vector sum of the p_T values of both tracks and of all reconstructed neutral particles, evaluated in the event CM frame.

The pion-impostor candidates ϕ are reconstructed by combining two photons, each with a CM energy larger than 250 MeV. To reduce the contribution of radiative events, we require the sum of the CM energies of all photons in the event not associated with the ϕ candidate to be less than 300 MeV. The latter requirement also has the effect of rejecting events containing more than one ϕ candidate. The photons associated with a ϕ candidate must be separated from the electron track by at least 30° to further suppress radiative events. Control samples of $\tau^\pm \to X^\pm(\pi^0)\nu_\tau$ events with $X^\pm = \pi^\pm$, $K^\pm$, $\mu^\pm\nu_\mu$ are used to determine momentum-dependent corrections for the ϕ selection efficiency [22].

Kinematic constraints are used to ensure that the ϕ candidate does not arise from events in which one τ lepton decays leptonically, while the other decays through $\tau^\pm \to \rho^\pm\nu$ followed by $\rho^\pm \to \pi^\pm\pi^0$, where the $\pi^\pm$ is misidentified as a lepton. We form the invariant mass between each track and the ϕ candidate, assuming a $\pi^\pm$ mass hypothesis for the track, and require the combined mass to be greater than the τ-lepton mass. To further suppress neutral pions from τ-lepton decays, the sum of the CM energy of the ϕ candidate, E_ϕ, and that of the track with the lower energy, $E_{\rm small}$, must be greater than $\sqrt{s}/2$. The distribution of $E_{\rm small} + E_\phi$ for events with $m_{\gamma\gamma} \in [100, 160]$ MeV/c^2, after all other selection criteria have been applied, is shown in Fig. 3.

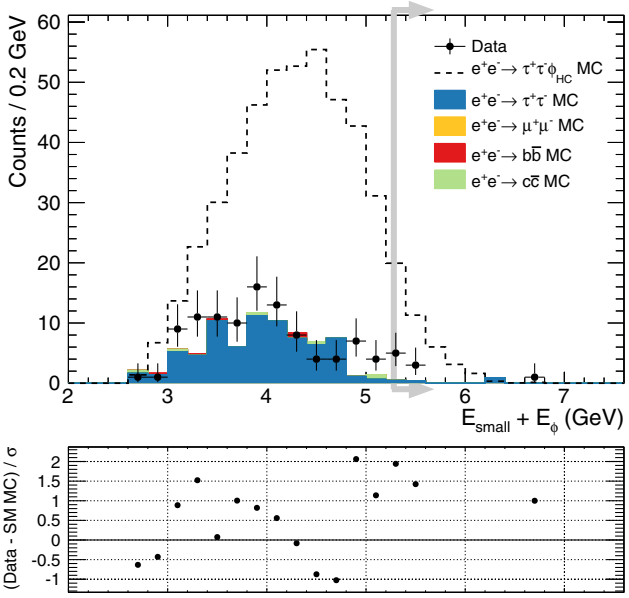

FIG. 3 (color online). Top: sum of the smaller of the track energies $E_{\rm small}$ and of the ϕ candidate energy E_ϕ, evaluated in the event CM, after applying all other selection criteria and requiring $m_{\gamma\gamma} \in [100, 160]$ MeV/c^2. The data to the right of the vertical line at 5.29 GeV are in the signal region. The predicted hardcore pion $e^+e^- \to \tau^+\tau^-\pi^0_{\rm HC}$ distribution, assuming a production cross section of 0.254 pb, is included for reference. Bottom: Difference between data and Standard Model simulation (SM MC), divided by combined statistical uncertainty.

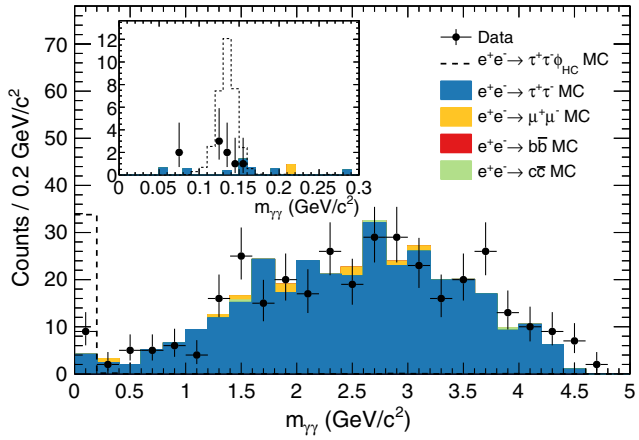

FIG. 4 (color online). Distribution of $m_{\gamma\gamma}$ after applying all other selection criteria. The insert shows the low mass range with bin size of 10 MeV$/c^2$.

The resulting diphoton mass spectrum after applying all other selection criteria is displayed in Fig. 4. The data are seen to agree with the SM simulation to within the uncertainties.

B. Yield extraction, background evaluation, and selection efficiency

The signal yield is extracted by performing a series of extended unbinned maximum likelihood fits to the diphoton invariant mass distribution in the $[50, 300]$ MeV$/c^2$ range, scanning ϕ mass hypotheses as explained below. This region is chosen because it includes the predicted mass range for the signal, and also because the background distribution is relatively flat. The $m_{\gamma\gamma}$ distribution is fitted with the sum of a Gaussian function, describing the contribution of the signal and peaking background components, and a first-order polynomial representing the combinatorial background. The number of events in the Gaussian peak is denoted N_g. The slope and normalization of the polynomial as well as the value of N_g are determined in the fit. The mean μ_g and width σ_g of the Gaussian function are fixed to values determined as explained below.

The value of σ_g is evaluated using control samples. These samples are selected, for both data and simulation, using criteria similar to those described above, but reversing the requirements on the invariant mass formed from the charged track and the π^0 candidate, and removing the requirement on $E_{\rm small} + E_\phi$. The reason this latter requirement is removed is to increase the statistical precision. The $m_{\gamma\gamma}$ spectra are then fitted using the signal model described above except with σ_g a fitted parameter. We find $\sigma_g = 10.6 \pm 1.8$ MeV$/c^2$ for the data and $\sigma_g = 11.2 \pm 0.8$ MeV$/c^2$ for the simulation. For the subsequent fits, we fix σ_g to 11.1 MeV$/c^2$, which is the average of the results from data and simulation.

The value of μ_g represents the mass of the hypothetical ϕ particle. It is fixed in the fit and scanned between 110 and 160 MeV$/c^2$, covering the expected range of impostor mass values [8]. The step size is 0.5 MeV$/c^2$, corresponding to less than half the estimated mass resolution.

We select the scan point that yields the largest value $N_g^{\rm max}$ of N_g. The signal yield $N_{\rm sig}$ is obtained by subtracting the estimated number of peaking background events from $N_g^{\rm max}$ and correcting for the signal yield bias.

The number of peaking background events predicted by the simulation is 0.38 ± 0.09, where the uncertainty accounts for uncertainties in the PID as well as for the difference between the data and simulation rates in the sidebands, which is visible in Fig. 3 for values of $E_{\rm small} + E_\phi$ above 4.8 GeV$/c^2$.

We also consider potential peaking backgrounds that are not present in the simulation. Specifically, we consider two-photon $e^+e^- \to e^+e^-\pi^+\pi^-\pi^0$ events, for which either the e^+ or e^-, and one of the charged pions, are undetected, while the other charged pion is misidentified as a muon. The events are selected using the same criteria as described above except requiring the presence of a charged pion rather than a muon. The $m_{\gamma\gamma}$ spectrum of the selected events is fitted as described above, and the resulting value of N_g is scaled by the muon-to-pion misidentification rate of $(3.0 \pm 1.0)\%$. Adding the resulting value to the number of peaking events determined from simulation yields an estimate of 1.24 ± 0.37 events. This number is subtracted from $N_g^{\rm max}$ as described above.

The evaluation of the fit bias is performed using a large ensemble of pseudo-experiments. For this purpose, diphoton invariant mass spectra are generated to reproduce the combinatorial background with the number of combinatorial events drawn from a Poisson distribution whose mean equals the simulated result. A peaking component centered at the π^0 mass is added. The number of peaking events is drawn from a Poisson distribution with mean equal to one. Each peaking background event is then weighted by a number drawn from a Gaussian distribution whose mean and width are 1.24 and 0.37 events, respectively. We determine the bias for several values of the signal yield by further adding a known number of signal-like events to each experiment. Between 0 and 25 signal events are added to each pseudo-experiment, yielding an average fit bias of -0.06 ± 0.02 events.

The signal selection efficiency is determined by applying the analysis procedures to the simulated signal events. After accounting for the $\tau^- \to \mu^-\bar{\nu}_\mu\nu_\tau$ and the $\tau^- \to e^-\bar{\nu}_e\nu_\tau$ branching fractions [23], the efficiencies are found to be $\varepsilon_{\phi_P} = \varepsilon_{\pi^0_{\rm HC}} = (0.455 \pm 0.017)\%$ and $\varepsilon_{\phi_S} = (0.0896 \pm 0.0033)\%$, where the uncertainties are statistical. The efficiency to reconstruct the ϕ_S is smaller than that to reconstruct the ϕ_P and $\pi^0_{\rm HC}$ because the scalar particle tends to produce lower-energy impostor candidates that do not satisfy the selection criteria.

TABLE II. Contributions to the uncertainty of the efficiency (%) for the three models considered.

Source of uncertainty	$\phi_P, \pi^0_{\rm HC}$ (%)	ϕ_S (%)
MC sample size	3.5	3.7
π^0 efficiency	1.0	1.0
PID	0.5	0.5
Momentum scale	0.2	0.2
Momentum resolution	0.1	<0.1
Energy scale	2.0	2.0
Energy resolution	0.6	0.6
Total systematic uncertainty	4.2	4.4

IV. SYSTEMATIC UNCERTAINTIES

Sources of systematic uncertainty affecting the efficiency measurement include those associated with the π^0 and PID efficiency corrections, as well as differences between the data and simulation in the track momentum scale and resolution, and in the photon energy scale and resolution. These multiplicative uncertainties are summarized in Table II. The additive uncertainty contributions to the signal yield measurement are associated with the peaking background estimate and potential biases in the fit procedure. For the latter, we assign the full bias correction as a systematic uncertainty.

The uncertainty related to the π^0 reconstruction efficiency is evaluated by performing the analysis while varying the π^0 efficiency correction within its uncertainties. The PID uncertainty is 0.5%, estimated using high-purity control samples.

The uncertainties associated with the differences between the data and simulation for the track momentum scale and resolution are measured using $e^+e^- \to \mu^+\mu^-\gamma$ events. These samples are also used to determine the uncertainties related to the photon energy scale and resolution [24].

V. RESULTS

A. Data $m_{\gamma\gamma}$ spectrum

Figure 5 shows the yield N_g of events in the Gaussian peak, with its statistical uncertainty, as a function of the ϕ particle mass hypothesis. The largest value, $N_g^{\rm max} = 6.2 \pm 2.7({\rm stat})$ events, arises for $\mu_g = 136$ MeV/c^2. The fit result with this mass hypothesis is shown in the diphoton mass distribution of Fig. 6, where the contribution from the expected background is also presented. The probability of observing a signal of at least 6.2 events assuming a background-only hypothesis is estimated from the pseudo-experiments described in Sec. IV, which assume a mass $\mu_g \in [110, 160]$ MeV/c^2. The p-value is found to be $p_0 = 3.71 \times 10^{-2}$.

After subtraction of the peaking background and correction for the fit bias, the number of signal candidate events at $\mu_g = 136$ MeV/c^2 is found to be

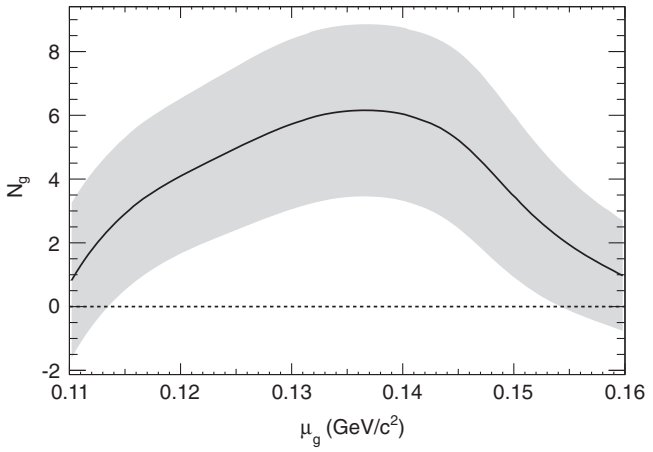

FIG. 5. Number N_g of events in the Gaussian peak as a function of the ϕ mass hypothesis μ_g. The shaded region indicates the statistical uncertainty.

$$N_{\rm sig} = 5.0 \pm 2.7({\rm stat}) \pm 0.4({\rm syst}). \quad (3)$$

Correcting this result for the signal selection efficiency leads to the following production cross sections:

$$\sigma = \begin{cases} 38 \pm 21({\rm stat}) \pm 3({\rm syst})\ {\rm fb} & \text{for } \phi_P \text{ and } \pi^0_{\rm HC}, \\ 190 \pm 100({\rm stat}) \pm 20({\rm syst})\ {\rm fb} & \text{for } \phi_S. \end{cases} \quad (4)$$

Statistical uncertainties dominate in both cases. The main source of systematic uncertainty is the peaking background estimation and subtraction procedure.

B. Upper limits on the cross sections

No significant signal is observed. Upper limits on the production cross sections are set using the CL_s method [25]. The 90% confidence level (CL) upper limit on the

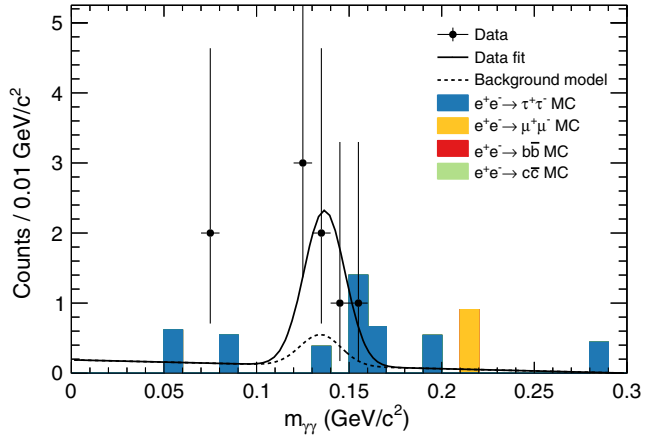

FIG. 6 (color online). Results for the $m_{\gamma\gamma}$ spectrum of the signal candidates. The solid line shows fit result for the signal and background model. The dotted line represents the contribution from background only using the linear component of the fit result added to the estimated peaking background of 1.24 events.

TABLE III. Consistency (p-value) of the measured production cross sections with the impostor theories adjusted to the *BABAR* $\mathcal{F}_{\pi^0}(Q^2)$ data.

Model	$\chi^2_{\min}$/n.d.f.		$\Delta\chi^2$/n.d.f.	p-value
	$\mathcal{F}_{\pi^0}(Q^2)$ and $\sigma_{e^+e^-\to\tau^+\tau^-\phi}$	$\mathcal{F}_{\pi^0}(Q^2)$ only		
$\pi^0_{\rm HC}$	23.7/10	11.9/9	11.8/1	5.9×10^{-4}
ϕ_P	48.4/10	10.8/9	37.6/1	8.8×10^{-10}
ϕ_S	49.2/10	13.4/9	35.8/1	2.2×10^{-9}

number of signal events, $N_{\rm sig} \leq 9.6$, translates into the following bounds on the cross section

$$\sigma \leq \begin{cases} 73 \text{ fb} & \text{for the } \phi_P \text{ and } \pi^0_{\rm HC} \text{ models,} \\ 370 \text{ fb} & \text{for the } \phi_S \text{ model.} \end{cases} \quad (5)$$

C. Compatibility of the measurement with the π^0 impostor theories

The compatibility of the measured production cross sections with the impostor theories is studied by including this measurement as an additional term in the χ^2 when calculating the optimal coupling values needed to describe the *BABAR* measurement of $\mathcal{F}_{\pi^0}(Q^2)$. The increase in χ^2 obtained when adding the couplings corresponding to our cross section measurements follows a χ^2 distribution with one degree of freedom. This is used to determine the p-values corresponding to a fluctuation of the $e^+e^- \to \tau^+\tau^-\phi$ event rate from the level seen in the present study to the level required to explain the *BABAR* $\mathcal{F}_{\pi^0}(Q^2)$ measurements.

The results are reported in Table III. As an example, the p-value for the hardcore pion model is found to be 5.9×10^{-4}, corresponding to a required fluctuation of 3.4 standard deviations. The p-values for the ϕ_P and ϕ_S models are on the order of 10^{-9}. Thus the pion impostor models do not provide a likely explanation for the excess seen in the *BABAR* pion-photon transition form factor data.

VI. SUMMARY

A search for π^0 impostors is conducted with the *BABAR* data set. At 90% confidence level, the limit on the production cross section in association with a $\tau^+\tau^-$ pair is 73 fb for the pseudoscalar impostor and the hardcore pion models, and 370 fb for the scalar impostor model. The p-values of our measurements under these hypotheses are 5.9×10^{-4} or smaller. The pion impostor hypotheses are disfavored as explanations for the nonasymptotic behavior of the pion-photon transition form factor observed with the *BABAR* data.

ACKNOWLEDGMENTS

We are grateful for the excellent luminosity and machine conditions provided by our PEP-II colleagues, and for the substantial dedicated effort from the computing organizations that support *BABAR*. The collaborating institutions wish to thank SLAC for its support and kind hospitality. This work is supported by DOE and NSF (USA), NSERC (Canada), CEA and CNRS-IN2P3 (France), BMBF and DFG (Germany), INFN (Italy), FOM (The Netherlands), NFR (Norway), MES (Russia), MINECO (Spain), STFC (United Kingdom), BSF (USA-Israel). Individuals have received support from the Marie Curie IEF program (European Union) and the A. P. Sloan Foundation (USA).

[1] B. Aubert *et al.* (*BABAR* Collaboration), Phys. Rev. D **80**, 052002 (2009).
[2] A. P. Bakulev, S. V. Mikhailov, A. V. Pimikov, and N. G. Stefanis, Phys. Rev. D **86**, 031501 (2012).
[3] A. Dorokhov, JETP Lett. **91**, 163 (2010).
[4] W. Lucha and D. Melikhov, J. Phys. G **39**, 045003 (2012).
[5] S. Noguera and V. Vento, Eur. Phys. J. A **46**, 197 (2010).
[6] S. J. Brodsky, G. P. Lepage, and P. B. MacKenzie, Phys. Rev. D **28**, 228 (1983).
[7] S. Uehara *et al.* (Belle Collaboration), Phys. Rev. D **86**, 092007 (2012).
[8] D. McKeen, M. Pospelov, and J. M. Roney, Phys. Rev. D **85**, 053002 (2012).
[9] ϕ represents a new object not related to the $\phi(1020)$.
[10] L. Bergström, Z. Phys. C **14**, 129 (1982).
[11] L. Bergström, Z. Phys. C **20**, 135 (1983).
[12] B. Aubert *et al.* (*BABAR* Collaboration), Nucl. Instrum. Methods Phys. Res., Sect. A **479**, 1 (2002).
[13] B. Aubert *et al.* (*BABAR* Collaboration), Nucl. Instrum. Methods Phys. Res., Sect. A **729**, 615 (2013).
[14] J. P. Lees *et al.* (*BABAR* Collaboration), Nucl. Instrum. Methods Phys. Res., Sect. A **726**, 203 (2013).
[15] D. J. Lange, Nucl. Instrum. Methods Phys. Res., Sect. A **462**, 152 (2001).
[16] T. Sjöstrand, Comput. Phys. Commun. **82**, 74 (1994).
[17] S. Jadach, B. Ward, and Z. Wąs, Comput. Phys. Commun. **130**, 260 (2000).
[18] S. Jadach, Z. Wąs, R. Decker, and J. H. Kühn, Comput. Phys. Commun. **76**, 361 (1993).
[19] S. Jadach, W. Płaczek, and B. Ward, Phys. Lett. B **390**, 298 (1997).

[20] E. Barberio and Z. Wąs, Comput. Phys. Commun. **79**, 291 (1994).
[21] S. Agostinelli *et al.*, Nucl. Instrum. Methods Phys. Res., Sect. A **506**, 250 (2003).
[22] A. Adametz, Ph.D. thesis, Ruperto-Carola University of Heidelberg, Germany, 2011.
[23] J. Beringer *et al.* (Particle Data Group), Phys. Rev. D **86**, 010001 (2012).
[24] B. Aubert *et al.* (*BABAR* Collaboration), Phys. Rev. Lett. **105**, 051602 (2010).
[25] A. L. Read, J. Phys. G **28**, 2693 (2002).